

# In-Plane Lunar Injection Opportunities from an Orbiting Space Station

WILLIAM R. WELLS\*

NASA Langley Research Center, Hampton, Va

## Nomenclature

- $i$  = inclination of earth satellite orbit plane to earth's equatorial plane  
 $J$  = coefficient of second harmonic of earth's gravitational potential  
 $r$  = radial distance of vehicle from center of earth  
 $R$  = equatorial radius of earth  
 $t$  = time measured from the nominal  
 $T$  = times for in plane injection opportunities  
 $\delta_M$  = inclination of moon's orbit to earth's equatorial plane  
 $\phi$  = inclination of earth satellite orbital plane to the earth-moon plane  
 $\Delta\phi$  = regression rate of earth satellite orbital plane about polar axis of earth  
 $\omega$  = angular velocity of moon  
 $\Omega_E$  = angle measured in equatorial plane from moon's ascending node to node of earth satellite orbital plane and equatorial plane  
 $\Omega_M$  = angle measured in earth-moon plane from moon's ascending node to node of earth satellite orbital plane and earth-moon plane

THE manner in which a near-earth satellite orbital plane regresses about the polar axis has been well established, e.g., see Ref. 1. In the event that a lunar launch is to be made from an earth satellite orbit (the injection to be made in the plane of this earth satellite orbit), a delay in injection will cause the lunar trajectory, due to this regression, to be established in a plane having an orientation in space different from that originally planned. Consequently, the moon, in general, will not be at the nodal point of the earth satellite orbital and earth-moon planes at the time the vehicle arrives there. It is possible to correct for the effects of this regression by the application of a velocity increment to change the plane of the lunar trajectory, as discussed in Ref. 2. If the delays, however, are to be of the order of days, as might be the case for a space station, then it is of interest to know that there are certain discrete intervals of time, after the nominal, in which injection into the lunar trajectory can be accomplished in the plane of the earth satellite orbit. These opportunities correspond to times for which the moon and either nodal point of the earth satellite orbital and earth-moon plane line up. Since the two motions are in opposite directions, this alignment occurs whenever the total angular travel of the moon and the node of the earth-moon plane and earth satellite orbital plane add up to  $180^\circ$ . The determination of these injection opportunities for all nominal positions of the moon in its orbit (all nominal values of  $\Omega_M$  in Fig. 1) is the object of this paper.

If  $\Omega_E$  and  $\Omega_M$  denote the location of the regressed node of the earth satellite orbital and the node of the earth-equatorial and earth-moon planes, respectively, measured from the moon's ascending node in the direction of regression, it is obvious from Fig. 1 that

$$\Omega_M = \cot^{-1} \left[ \frac{\cos \delta_M \cos \Omega_E - \sin \delta_M \cot i}{\sin \Omega_E} \right] \quad (1)$$

where

$$0 \leq \Omega_E \leq 360 \quad 0 \leq \Omega_M \leq 360$$

If at time  $t = 0$  (the nominal time of injection from earth orbit)  $\Omega_M = (\Omega_M)_0$  and  $\Omega_E = (\Omega_E)_0$ , then, after a time in earth orbit of  $t = T$ , the nodal point of the earth satellite orbital

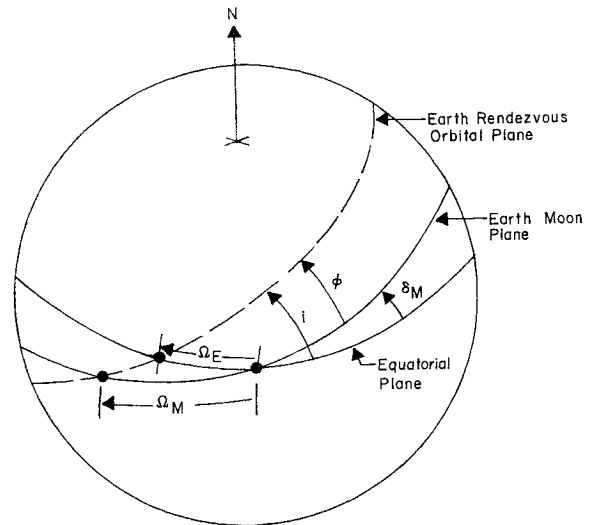


Fig. 1 Illustration of pertinent angles

and earth-equatorial planes will have regressed an amount  $\Delta\Omega_E$  along the earth-equatorial plane, and the nodal point of the earth satellite orbital and earth-moon planes will have regressed an amount  $\Delta\Omega_M$  along the earth-moon plane. Therefore, at time  $t = T$ ,

$$\Omega_M = (\Omega_M)_0 + \Delta\Omega_M \quad \Omega_E = (\Omega_E)_0 + \Delta\Omega_E$$

The regression rate of the node along the earth-equatorial plane is constant and for circular orbits is

$$\Delta\phi = 2\pi J \cos i (R^2/r^2) \quad (2)$$

Then, after time  $T$ ,

$$\Delta\Omega_E = T\Delta\phi \quad \Omega_E = (\Omega_E)_0 + T\Delta\phi \quad (3)$$

The corresponding value of  $\Omega_M$ , in terms of  $T$ , is obtained by substitution of Eq. (3) into Eq. (1). Therefore, at  $t = 0$ ,

$$\Omega_M = (\Omega_M)_0 = \cot^{-1} \left[ \frac{\cos \delta_M \cos (\Omega_E)_0 - \sin \delta_M \cot i}{\sin (\Omega_E)_0} \right]$$

and at time  $t = T$

$$\Omega_M = \cot^{-1} \left( \frac{\cos \delta_M \cos [(\Omega_E)_0 + T\Delta\phi] - \sin \delta_M \cot i}{\sin [(\Omega_E)_0 + T\Delta\phi]} \right) \quad (4)$$

The determination of the time increments for the in plane injection opportunities is accomplished by a solution for  $T$  of the equation

$$\Delta\Omega_M + \omega T = 180 \quad \text{or} \quad \Omega_M - (\Omega_M)_0 + \omega T = 180 \quad (5)$$

where  $\omega$  is the angular rate of the moon in its orbit (about  $13.2^\circ/\text{day}$ ).

It is of considerable interest in such an operation as this to know the manner in which the inclination of the trajectory plane to the earth moon plane varies for each injection opportunity. This inclination is designated by the angle  $\phi$  in Fig. 1. From Fig. 1, it is obvious that

$$\phi = \sin^{-1} (\sin i \sin \Omega_E / \sin \Omega_M) \quad (6)$$

Then, if an injection opportunity occurs  $T$  days after the nominal, substitution of  $\Omega_E$  from Eq. (3) and  $\Omega_M$  from Eq. (4) into Eq. (6) will give the inclination of the trajectory plane to the earth moon plane for this injection opportunity. This variation can be considerable, as will be pointed out below when a particular numerical example is illustrated.

To illustrate the significance of Eqs. (5) and (6), a numerical example is represented in Fig. 2 for the case of  $\delta_M = 28.5^\circ$ ,  $i = 30^\circ$ , and  $r = 315$  statute miles. Figure 2 gives the first few in-plane injection opportunities as a function of the

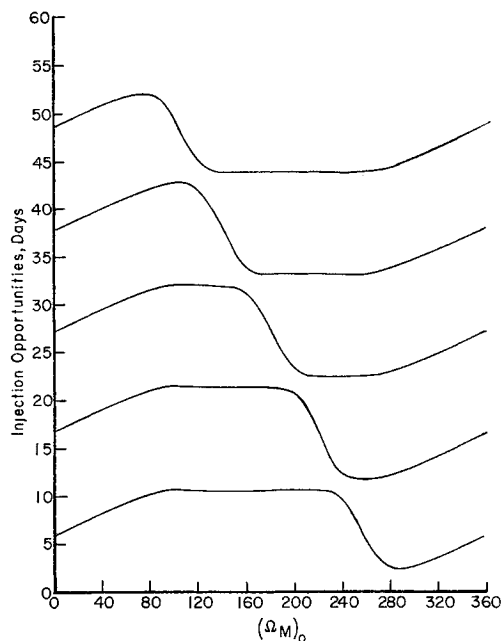


Fig 2 In-plane injection opportunities for all nominal lunar positions

nominal values of  $\Omega_M$ . These curves show that for the majority of the nominal injection conditions the opportunities for injection, after the first opportunity, occur about every 10.5 days. The variations in  $\phi$  at the injection opportunities for this case is between  $1.5^\circ$  and  $58.5^\circ$ .

#### References

- <sup>1</sup> Blitzer, L., "Apsidal motion of an IGY satellite orbit," *J Appl Phys* **28**, 1362 (1957)
- <sup>2</sup> Wells, W. R., "The influence of precession of earth rendezvous orbits on lunar mission requirements," NASA TN D-1512 (1962)

## A Calorimeter Study of a Magnetically Stabilized Arc-Heater

ROGER B STEWART\*

NASA Langley Research Center, Hampton, Va

#### Nomenclature

- $A$  = area,  $\text{ft}^2$   
 $C_d$  = nozzle discharge coefficient,  $\dot{m}_{\text{actu}} / \dot{m}_{\text{ideal}}$   
 $d$  = throat diameter, in  
 $h$  = enthalpy, Btu/lb  
 $\dot{m}$  = mass flow rate, lb/sec  
 $p$  = pressure, psi  
 $T$  = temperature,  $^\circ\text{R}$   
 $u$  = velocity, fps  
 $\gamma$  = ratio of specific heats,  $C_p/C_v$   
 $\rho$  = density,  $\text{lb}/\text{ft}^3$

#### Superscript

- \* = sonic throat conditions

#### Subscripts

- cold = arc off running conditions  
hot = arc on running conditions  
t = total conditions

#### Introduction

TEMPERATURES in the stagnation chambers of arc-heated wind tunnels are often obtained by means of a sonic throat analysis using measured values of stagnation pressure, mass flow, and throat area. A recent study of the total energy of air exhausting from a magnetically stabilized arc-heater indicates that, if the effective throat area is taken as being equal to the geometric throat area in the sonic flow analysis, large errors in stagnation enthalpy determination can result. Within a properly selected range of operating conditions, a particular form of the sonic flow relations can be used to give good agreement with the calorimeter results.

#### Experimental Apparatus

The facility used for this investigation was a modified version of the arc-heater described in Ref 1. The heater employed a 12,000 gauss magnetic field to rotate the arc between a center cathode and the cylindrical walls of the arc chamber (anode). The heater had a 4-in long arc chamber and a  $2\frac{1}{2}$ -in-long plenum chamber, which was followed by a separately cooled converging-diverging nozzle section. The supersonic flow (Mach number  $\approx 2$ ) from the nozzle was discharged into a water-cooled calorimeter and then exhausted to atmosphere. Figure 1 is a diagram of the apparatus used. Three separate nozzle sections were used having throat diameters of 0.125, 0.137, and 0.210 in. Two cathode designs were used with the 0.210-in throat and are also shown in Fig 1.

Cooling water temperatures in the calorimeter lines were measured with calibrated thermocouple probes immersed in the flow and were read on manually balanced precision potentiometers. Water mass flow rates in the calorimeter were measured with a precision bore flowmeter calibrated after being installed in the calorimeter system. Air mass flow rates were measured with a calibrated orifice using a differential pressure transducer and an oscillograph. The temperature of the air exhausting from the calorimeter was measured with a total temperature probe and read on a Brown recorder. Profiles of the exit air temperature were obtained for all reported data, and a check of total pressure across the calorimeter exit showed a variation of less than  $\frac{1}{4}\%$  of centerline pressure between the centerline and outer wall. Measured heat losses from the calorimeter to room air amounted to 1% of the total heat flux through the calorimeter, and a correction was made in the data reduction for these losses. Heat losses to the nozzle section were obtained by measuring water flow rates through the section with turbine type flowmeters, and temperature changes were measured with thermocouples immersed in the cooling lines. It is felt that the uncertainty of the entire calorimeter and air mass flow system was no more than  $\pm 6\%$ .

#### Sonic Throat Technique

A currently useful means of obtaining stagnation chamber enthalpy levels is through use of a sonic throat analysis. By the assumption of a one-dimensional, isentropic expansion from stagnation chamber to sonic throat conditions, the stagnation enthalpy can be related to the stagnation pressure, the mass flow, and the effective throat area. A plot of this relationship for high-temperature air appears as chart 14 of Ref 2. In a similar fashion, a straight line fit to a plot of  $\log(p_{t, \text{hot}} A^*_{h, t} / \dot{m}_{\text{hot}})$  vs  $\log h^*$  can be used to give the following equation:

$$h^* = 0.00645 \left[ \frac{p_{t, \text{hot}} A^*_{h, t}}{\dot{m}_{\text{hot}}} \right]^{2.48} \text{ Btu/lb} \quad (1)$$

If it is assumed that  $A^*_{h, t} = A^*_{g, \text{om t i}}$ , measured values of stagnation pressure and the mass flow will then determine the sonic enthalpy in Eq (1) ( $h_t$  can easily be obtained from  $h^*$ ). Cold, perfect gas ( $\gamma = 1.4$ ) relations can be introduced in

Received November 15, 1963

\* Aerospace Engineer Member AIAA